A PINTO POINT ASSEMBLAGE FROM CA-INY-134 ("AYERS ROCK"), INYO COUNTY, CALIFORNIA

ALEXANDER K. ROGERS
MATURANGO MUSEUM

ROBERT M. YOHE II
CALIFORNIA STATE UNIVERSITY, BAKERSFIELD

The Ayers Rock site (INY-134) is located in southern Inyo County, California, on the northwestern edge of the Coso Volcanic Field. Excavated in the 1960s, the site yielded 130 projectile points, of which 31 are Pinto. In this article we report an obsidian hydration age computation on the Pinto points and their metric data, and compare the metrics with previously reported Pinto points from this region. The Pinto points from this site exhibit an age of 5684 ±1445 cal B.P. (n = 16), based on obsidian hydration dating. Metrics are compared with those from 11 other Pinto sites in California and Nevada, and suggest possible cultural contact with peoples from the desert regions around Ft. Irwin.

The Ayers Rock site (CA-INY-134) is located on land managed by the BLM in southern Inyo County, California, on the northwestern edge of the Coso Volcanic Field (Figure 1). The site is named for a house-size boulder bearing red, white, and black pictographs that visually dominates the area of the site. The site was excavated around 1960 by the Archaeological Survey Association of Southern California (Redfeldt 1962), but the collection was subsequently lost. It was relocated in 1998 through the efforts of Russell Kaldenberg, then California State Archaeologist for the BLM, and Daniel McCarthy of the U.S. Forest Service. The collection and field notes were analyzed by David Whitley and colleagues, and a report was published through the Maturango Museum (Whitley et al. 2005).

The artifact collection from Ayers Rock includes basketry, cordage, ceramics, lithics, and human remains. Whitley et al. (2005) reported on the totality of the artifact collection, but were limited by its condition. Very few field notes existed, and documentation was largely limited to notes written on containers. Chronological analysis was based entirely on temporally sensitive artifacts, plus 17 obsidian hydration dates. The collection is curated at the Maturango Museum for the BLM.

In 2005, Judyth Reed, then archaeologist at the BLM Ridgecrest Field Office, suggested the authors undertake a more detailed analysis of the Pinto points from the site (n = 31). This article reports the results of the analysis, including mathematical analyses of stratigraphy, materials, metrics, and manufacturing technology. Hydration dates are reported for 17 of the Pinto points. Metrics for the Pinto points are compared with data reported by Basgall and Hall (2000) for 11 sites in Nevada and eastern California.

SITE

The site consists of three principal loci, denoted Shelters 1, 2, and 3; additional smaller loci were identified in the field notes, but subsequent efforts could not locate them (Whitley et al. 2005) (Figure 1). Shelter 1, which is actually an open-air locus, was located immediately east of the pictograph boulder (Figure 2), while Shelter 2 was a rock shelter in a boulder field to the northeast. Shelter 3 was also a rock shelter, located to the northwest, also in a boulder field (Figure 1). Projectile points were recovered principally from the three shelter loci, with a few additional of unknown provenience.

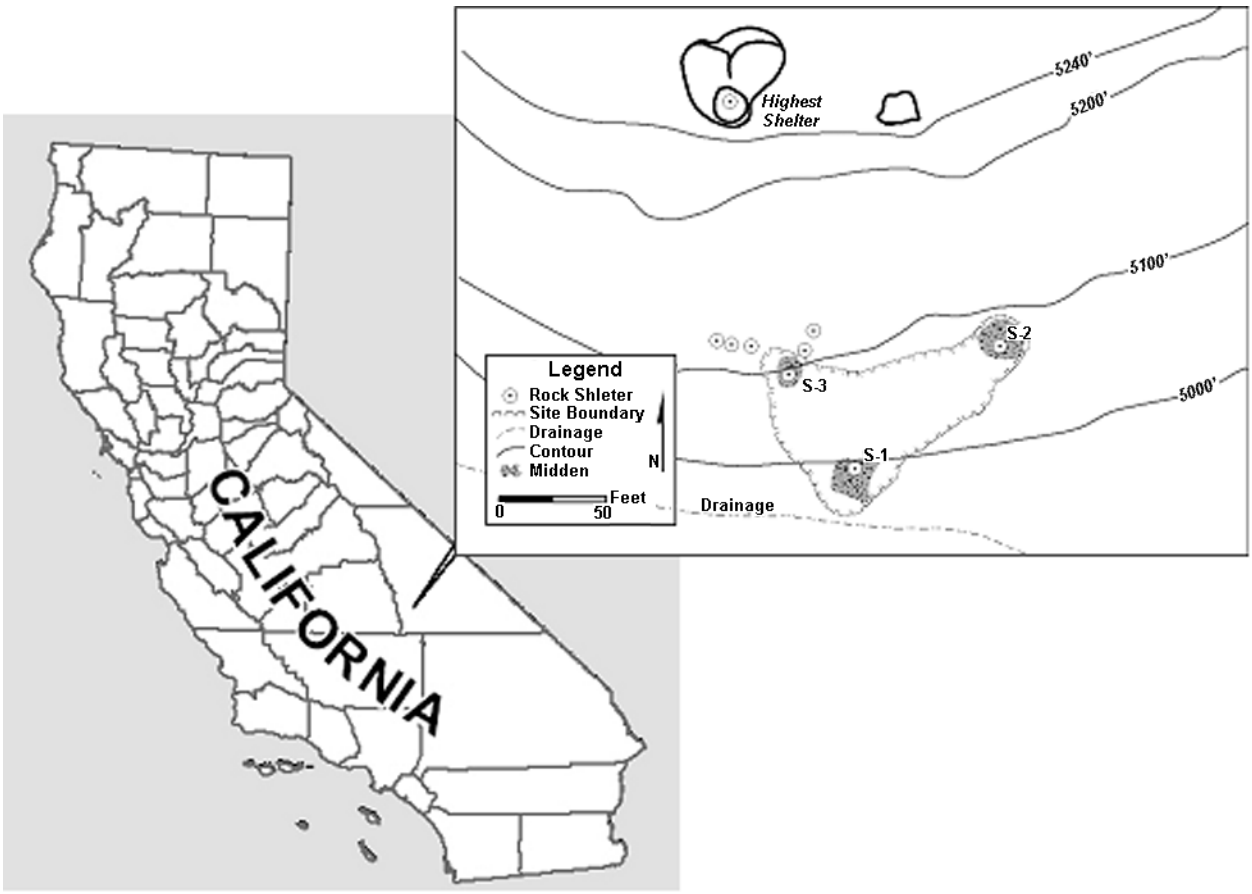

Figure 1. INY-134, site location and shelter loci. Locus map from Whitley et al. 2005.

Figure 2. Boulder at Locus 1, and pictograph panel on northeast side. The boulder is approximately 7 m high.

Table 1. Projectile point types at INY-134.

TYPE	N
Cottonwood Triangular	16
Desert Side-Notched	7
Rose Spring	29
Eastgate	3
Elko	20
Humboldt	11
Pinto	31
Silver Lake	3
Lake Mohave	1
Unidentified	9
Total	130

Table 2. Geochemical sources of the obsidian projectile points, INY-134.

SOURCE	N	%
West Sugarloaf (WSL)	31	60
Sugarloaf Mountain (SLM)	10	19
West Cactus Peak (WCP)	8	15
Joshua Ridge (JRR)	3	6
Total	52	100

Table 3. Projectile point distribution, INY-134.

LOCUS	CWT	DSN	RS	EG	ELKO	HUMB	PINTO	SL	LM	UNID.	TOTAL
Shelter 1	2	2	5	--	2	2	29	2	--	2	46
Shelter 2	2	--	5	1	10	2	1	1	--	1	23
Shelter 3	9	5	16	1	8	6	1	--	--	4	50
Unknown	3	--	3	1	--	1	--	--	1	2	11
Total	16	7	29	3	20	11	31	3	1	9	130

PROJECTILE POINT ASSEMBLAGE

A total of 130 projectile points were recovered from the site, spanning the time from Great Basin Stemmed to Desert series; Table 1 summarizes point types. A total of 52 of the obsidian points, spanning all point types, were subjected to geochemical sourcing by X-ray fluorescence (XRF; see Northwest Research Obsidian Studies Laboratory 2008). The majority (60 percent) are from the West Sugarloaf source, with significantly smaller fractions from Sugarloaf Mountain, West Cactus Peak, and Joshua Ridge (Table 2). However, the apparent preference for West Sugarloaf obsidian is probably due more to its ubiquity and the widespread extent of the flow than to any perception of superior material properties.

The points were recovered primarily from three loci, Shelters 1, 2, and 3, as summarized in Table 3 (total = 130; nine of the total are of unknown provenience).

MATERIALS ANALYSIS

Projectile points from INY-134 were manufactured from obsidian, cryptocrystalline silica, and basalt. Data are summarized in Table 4 for the site; there are no consistent differences between loci. Figure 3 shows that obsidian has been the preferred material for all point types represented. It is especially notable that the Desert series points (CWT/DSN) and the Pinto points are entirely obsidian and

Table 4. Projectile point material at INY-134.

Material	Great Basin Stemmed	Pinto	Humboldt	Elko	Rose Spring / Eastgate	Cottonwood Triangular / Desert Side-notched	Unidentified	Total
Basalt	1	--	--	--	--	--	--	1
Cryptocrystalline silica	1	--	--	4	3	--	1	9
Obsidian	2	31	11	16	29	23	8	120
Total	4	31	11	20	32	23	9	130

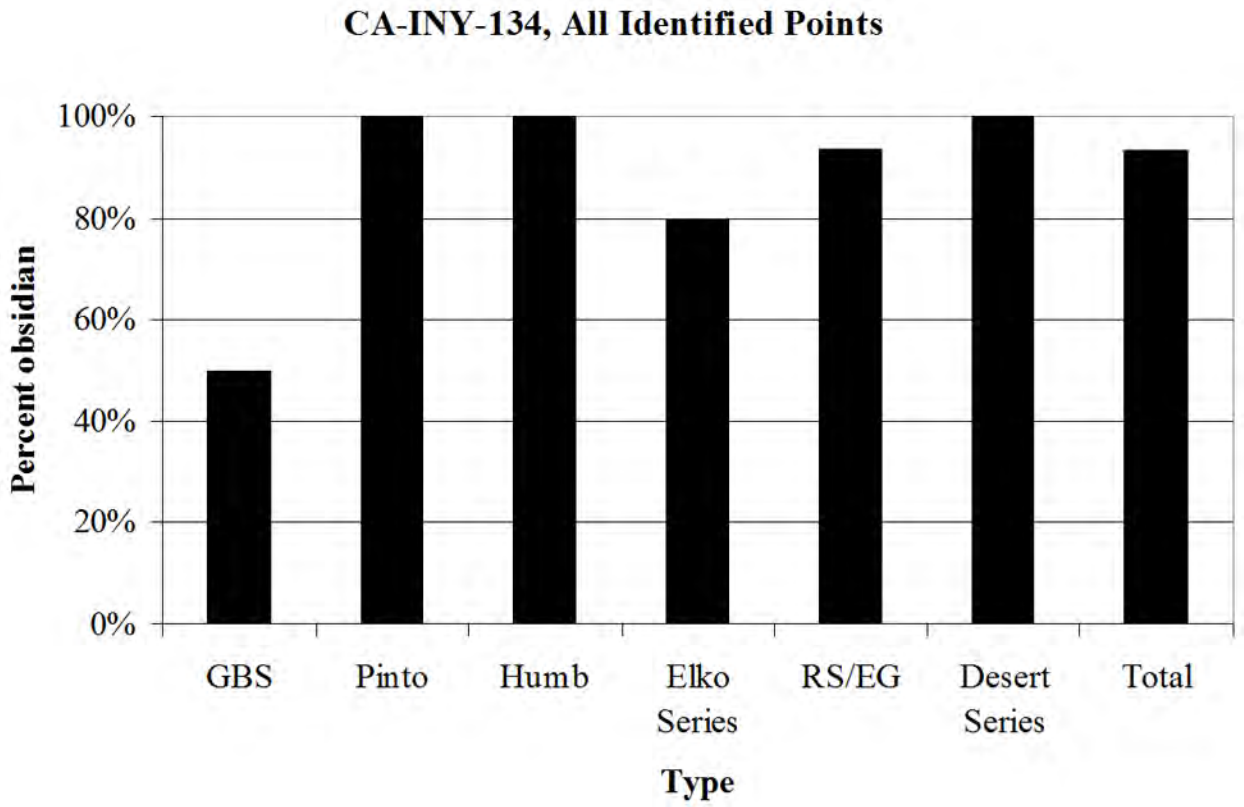

Figure 3. Percentage of obsidian employed in each point type at INY-134.

have large sample sizes. The anomalies are the Great Basin Stemmed series (50 percent obsidian) and Elko (75 percent obsidian). The Great Basin Stemmed series is represented by a very small sample size and, in one case, uncertain provenience. The Elko series, which has a reasonable sample size (n = 20), employs 25 percent cryptocrystalline silica, more than the others, for reasons which are not clear. One of the Eastgate points (Cat. No. 672) is very finely manufactured of cryptocrystalline silica, representing one-third of the Eastgate sample.

In summary, the material used in manufacture was overwhelmingly obsidian. The predominance of obsidian over basalt and cryptocrystalline silica is not surprising, since the site is located only 11 km

Figure 4. Pinto point collection from INY-134; point cat. no. 631 was unavailable for photographing. Note the careful pressure flaking on some of the points.

northwest of the West Sugarloaf obsidian sources of the Coso Volcanic Field. (By contrast, the Stahl site, INY-182, is located 9 km southwest of West Sugarloaf; the distance between the two sites is 18 km.)

PINTO POINTS - STRATIGRAPHIC ANALYSIS

The Pinto point assemblage is shown in Figure 4. Stratigraphic details of the entire projectile point assemblage are presented by Whitley et al. (2005). The analysis here focuses on only the Pinto points, the bulk of which (29 out of 31) are from Shelter 1. Figure 5 shows the cumulative distribution with depth of the Pinto points and of the Rose Spring/Eastgate points from Shelter 1. The two distributions are not distinguishable at the 95 percent confidence level (max. delta = 0.421; threshold = 0.659; the high threshold is due to the relatively small sample size for Rose Spring points). The fact that

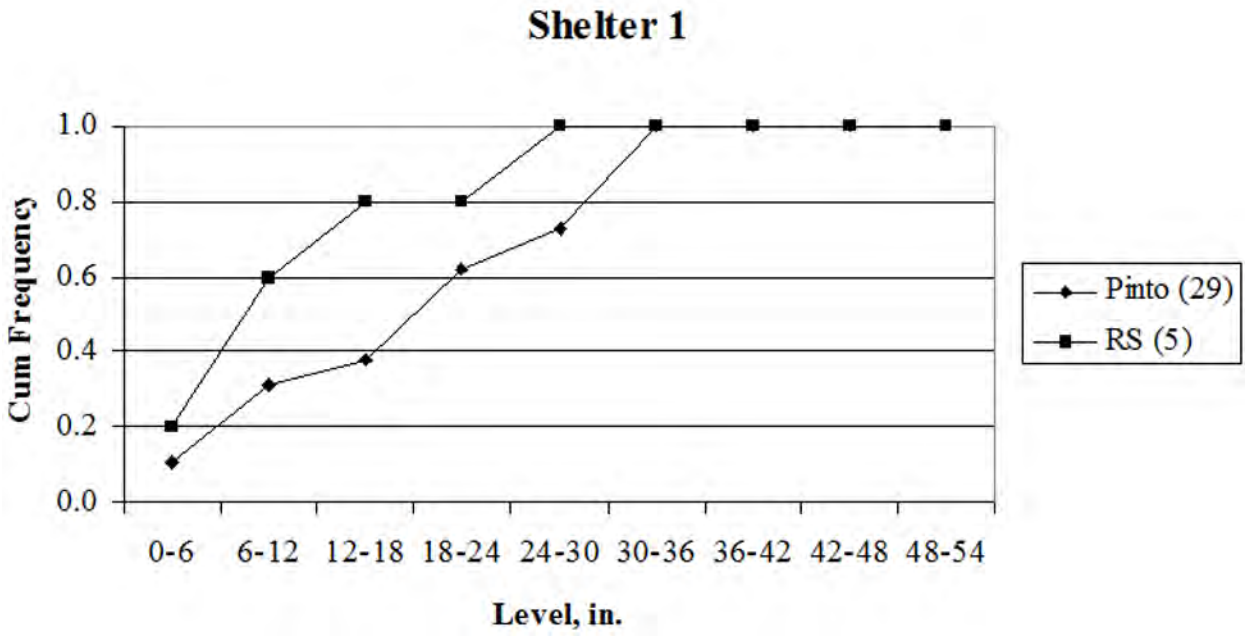

Figure 5. Cumulative distributions of Rose Spring (RS) and Pinto points by level at Shelter I, INY-134. The distributions are not statistically distinguishable.

Table 5. Coso obsidian hydration rates at 20°C.

FLOW	RATE (μ^2 / 1,000 YRS.)	RATE CV
Sugarloaf Mtn. (SLM)	29.87	0.11
West Sugarloaf (WSL)	18.14	0.12
West Cactus Peak (WCP)	27.28	0.46
Joshua Ridge (JRR)	22.27	0.25
Coso Volcanic Field	22.86	0.33

the distributions are statistically indistinguishable may suggest that significant turbation has occurred at the site, which is taken into account in the obsidian hydration analysis, below.

HYDRATION DATING

Method

Three general classes of methods have been proposed for measuring obsidian hydration: measurement of water mass uptake or loss vs. time (Ebert et al. 1991; Stevenson and Novak 2011), direct measurement of water profiles vs. depth (Anovitz et al. 1999, 2004, 2008; Riciputi et al. 2002; Stevenson et al. 2004), and observation of the leading edge of the stress zone by optical microscopy (many papers, e.g. Friedman and Smith 1960; Friedman and Evans 1968; Friedman and Long 1976).

The method used here is based on the last-named approach, i.e., classical obsidian hydration dating (OHD). Laboratory data (Rogers and Duke 2011; Stevenson and Scheetz 1989; Stevenson, Cartpenter, and Scheetz 1998; Stevenson, Mazer, and Scheetz 1998) indicate that the position of this stress zone, or hydration front, progresses into the obsidian proportional to t^n, where n is approximately 0.5 within limits of experimental error. The agreement with classical diffusion theory, in particular Fick's

formulations and the Boltzmann transformation (Crank 1975:105; Doremus 2002; Rogers 2007, 2012), may be a coincidence or may be due to an as-yet-undiscovered property of the hydration process itself.

The ages computed here are based on modeling the hydration process by temperature-dependent diffusion theory (Rogers 2007, 2012). The basic equation for age computations is

$$t = r_c^{\,2} / k \qquad (1)$$

where t is age, r_c is the hydration rim as corrected for effective hydration temperature (EHT), and k is the hydration rate.

The hydration rate is a function of temperature and also varies by flow within the Coso Volcanic Field and between sources (Rogers 2011). Table 5 shows the values used here, at a reference temperature of 20°C. If the flow is not known, the composite value for the volcanic field is used.

The hydration rate is affected by ground-water chemistry (Morgenstein et al. 1999), obsidian anhydrous chemistry (Friedman et al. 1966), obsidian intrinsic water content (Zhang and Behrens 2000; Zhang et al. 1991), humidity (Friedman et al. 1994; Mazer et al. 1991), and temperature (Rogers 2007). Ground-water chemistry is only a problem in cases where potassium content is very high, as in some desert playas; otherwise, it can be ignored. Obsidian anhydrous chemistry is controlled by sourcing the obsidian, and is a minor effect (Delaney and Karsten 1981; Karsten et al. 1982; Stevenson et al. 2000). Intrinsic water concentration can vary within an obsidian source (Stevenson et al. 1993) and can affect hydration rate significantly (Zhang et al. 1991; Zhang and Behrens 2000); there are no archaeologically appropriate techniques for measuring intrinsic water at present, so its effects must be controlled statistically, by sample size. Humidity has a small effect that can generally be ignored.

Temperature has the major effect, which needs to be controlled in performing an obsidian analysis. Archaeological temperatures vary both annually and diurnally, and the hydration rate is a strong function of temperature. Effective hydration temperature (EHT) is defined as a constant temperature which yields the same hydration results as the actual time-varying temperature over the same period of time. Due to the mathematical form of the dependence of hydration rate on temperature, EHT is always greater than or equal to the mean temperature. The mathematical derivation is given by Rogers (2007).

The solution for EHT is a numerical integration of the temperature-dependent hydration rate over a time span in which the temperature varies diurnally and annually about an annual mean temperature (Rogers 2007), accomplished for this analysis by a computer code in MatLab® 7.0. The temperature is modeled as the sum of a mean temperature and two sinusoids, one with a 24-hour period and the other with a 12-month period. The time increment is 1 hour, and the period of integration is 1 year. The temperature model thus requires specification of the constant term (annual average temperature) and the amplitude of the two sinusoids (annual variation and mean diurnal variation).

Most archaeological sites are not collocated with meteorological stations, but temperature parameters for them can be estimated by regional temperature scaling (Rogers 2008a). It is important to use long-term data in these computations, and 30 years is the standard for determining climatological norms (Cole 1970). Such data can be downloaded from the web site of the Western Regional Climate Center. The scaling principle is that desert temperature parameters are a strong function of altitude above mean sea level, and the best estimates of temperature are determined by scaling from 30-year data from a large number of meteorological stations. Using this technique, and a site elevation of 5,100 ft. amsl, the average annual temperature at INY-134 was computed to be 13.1°C, the annual variation (July mean minus January mean) is 20.6°C, and the mean diurnal variation is 15.8°C.

These are air temperatures. Obsidian on the surface is exposed to surface temperatures, which can be significantly higher than air temperatures in areas devoid of vegetation (Johnson et al. 2002; Rogers 2008b). However, a detailed analysis based on data from Rose Spring (INY-372) has been shown that meteorological air temperature gives a good estimate of surface ground temperature in situations in which even intermittent shade is present (Rogers 2008c).

Since climate has not been stable over periods of archaeological interest, the effects of resulting temperature changes must be included in some cases. West et al. (2007:15, Figure 2.2 C, D) show a reconstruction of the variation of regional-scale mean temperature since the late Pleistocene, based on multi-proxy data. Rogers (2010a) showed a method for computing a correction factor to adjust an OHD age based on current conditions to account for paleotemperature variations. The effect is relatively small, less than ±7 percent, for ages back to 18,000 years. The MatLab codes employed in this analysis include this paleotemperature correction.

For buried artifacts, V_a and V_d represent the temperature variations at the artifact burial depth, which are related to surface conditions by

$$V_a = V_{a0} \exp (-0.44\ z) \qquad (2a)$$

and

$$V_d = V_{d0} \exp (-8.5\ z) \qquad (2b)$$

where V_{a0} and V_{d0} represent nominal surface conditions and z is burial depth in meters (Carslaw and Jaeger 1959:81).

Depth correction for EHT is desirable, even in the presence of site turbation, because the depth correction, on the average, gives a better age estimate. The computer code used here accounts for the length of time an artifact was buried, as well as the depth, based on a user-input value of the fraction of that artifact life that it was buried. The algorithm computes an average value of the diffusion coefficient over time and uses this value to compute age. Because of the obvious turbation that has occurred, the assumption is made that the artifact was buried for half its life at its recovery depth, and spent the other half of its life on the surface.

Once EHT has been computed, the measured rim thickness is multiplied by a rim correction factor (RCF) to adjust the rims to be comparable to conditions at a reference site:

$$RCF = \exp [(E / EHT_r) - (E / EHT)] \qquad (3)$$

where EHT_r is effective hydration temperature for the hydration rate (20°C here) and E is the activation energy of the obsidian (assumed to be 10,000ºK for Coso). The EHT-corrected rim value r_c is then

$$r_c = RCF \times r \qquad (4)$$

This parameter is then used in equation 1 to compute the estimate of mean age.

There are always errors, or uncertainties, in the parameters used for age computation. The primary sources of error are obsidian rim measurement, errors in the hydration rate ascribed to a source, intra-source rate variability due to uncontrolled intrinsic water in the obsidian (Ambrose and Stevenson 2004; Rogers 2008d; Stevenson et al. 1993, 2000; Zhang and Behrens 2000; Zhang et al. 1991), errors in reconstructing the temperature history, and association errors caused by site formation processes (Schiffer 1987). The effects of these errors have been examined in detail, with the analysis documented by Rogers (2008d, 2010b).

Obsidian sample sizes are generally relatively small due to cost constraints, while the uncertainty sources produce at least five degrees of freedom in the errors. For this reason, sample standard deviation is generally not a good estimate of age accuracy; a better strategy for estimating age accuracy is to use a priori information about the individual error sources, and infer the accuracy of the age estimate. The mathematics to make this inference was developed by Rogers (2010a), and is summarized below.

The coefficient of variation of the age estimate, CV_t, can be shown to be

$$CV_t^2 = 4 [(\sigma_r / r)^2 + (0.06\ \sigma_{EHT})^2 + (CV_{ks} / 2)^2 + CV_{ke}^2] \qquad (5)$$

where the variables are defined as follows: σ_r is the standard deviation of the hydration rim measurement, and is ~ 0.1μ; r is the mean hydration rim; σ_{EHT} is the uncertainty in EHT post-correction, and is ~ 1.0°C; CV_{ke} is the coefficient of variation of the hydration rate ascribed to the obsidian source, and is typically ~ 0.05; and CV_{ks} is the coefficient of variation of the intra-source rate variations, with typical CV values as in Table 1.

Table 6. INY-134 projectile point ages computed by obsidian hydration dating.

Cat. No.	Type	Locus	Unit	Level (in.)	Source	Hydration (μ)	Age (cal B.P.)	Age Std. Dev. (cal yrs.)
73	Pinto	1	D11	24-30	SL	9.80	4997	960
74	Pinto	1	D11	24-30	WSL	9.10	6891	1366
116	Pinto	1	B9	0-6	SL	7.60	2871	554
137	Pinto	1	C11	0-6	WSL	7.60	4656	925
141	Pinto	1	C11	6-12	WSL	11.60	11226 *	2220
142	Pinto	1	C11	6-12	WSL	8.70	6075	1205
143	Pinto	1	C11	6-12	JR	8.70	5078	1501
147	Pinto	1	C11	6-12	WSL	10.00	8089	1602
157	Pinto	1	C11	18-24	WSL	8.20	5597	1111
168	Pinto	1	C11	30	SL	12.40	7875	1510
171	Pinto	1	C12	6-12	SL	12.10	7121	1366
174	Pinto	1	D11	18-24	WSL	8.90	6514	1291
175	Pinto	1	D11	30-36	WSL	8.60	6219	1234
176	Pinto	1	D11	30-36	WSL	6.40	3683	735
177	Pinto	1	D11	30-36	WSL	8.00	5462	1085
178	Pinto	1	D11	30-36	WCP	8.40	4194	2040
180	Pinto	1	D12	30	WCP	10.00	5624	2734

* Excluded from averages; possibly geologic.

Table 7. INY-134 projectile point age statistics, from obsidian hydration analysis.

N	Mean Rim (μ)	Rim Std. Dev. (μ)	Mean Age (cal B.P.)	Age Std. Dev. (cal yrs.)	Age CV
16	9.03	1.57	5684	1445	0.25

Once CV_t is computed from equation 5, the standard deviation of the uncertainty in the age estimate is

$$\sigma_t = CV_t \times t \qquad (6)$$

This is the accuracy figure quoted in the computer code output. The sample standard deviation is also provided for comparison, but is not very informative unless n >> 1.

Results

The computations are based on source data and hydration rim data provided by Northwest Research Obsidian Studies Laboratory (2008). Table 6 provides the age data as computed, and Table 7 and Figure 6 present age statistics for the Pinto points. These values agree reasonably well with expected ages (e.g., Haynes 2004; Justice 2002; Yohe 1998). The coefficient of variation (0.25) is typical of water content of Coso obsidians.

Two cautionary remarks are in order on analysis. Obsidian hydration dating has greatly improved over the past five years, but it is still subject to uncertainties. Two primary sources of uncertainty are the temperature history of the artifact and its intrinsic water content. Temperature history, in turn, depends on local climate and on site formation processes, notably burial history. The mathematical techniques used herein can correct for temperature to a major degree but are not perfect.

Also, the hydration rate of obsidian is a function of the intrinsic water content of the obsidian. This water is a result of original solidification of the magma, and is typically < 2 percent by weight. However, it has a major influence on hydration rate, and since it is very costly to measure, most archaeological work does not control for it. Sourcing by XRF provides a first level of control, since water

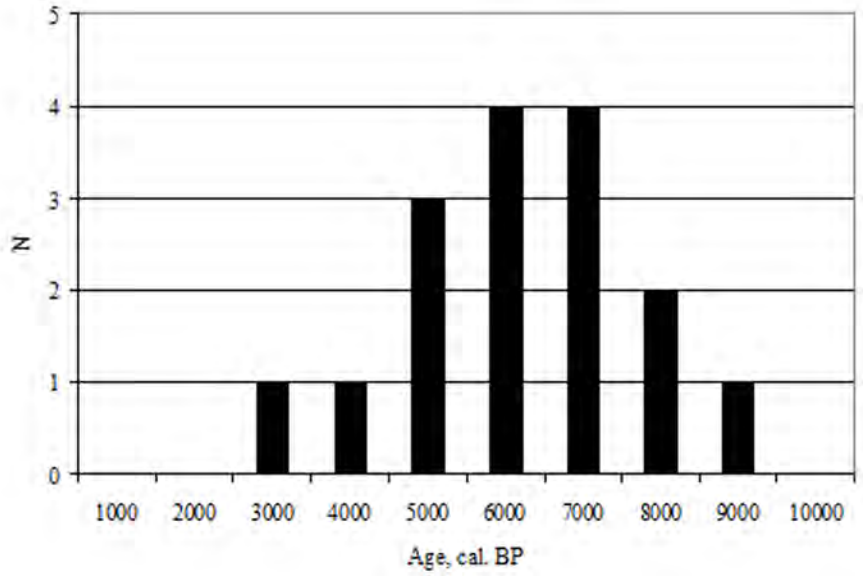

Figure 6. Obsidian hydration age distribution for Pinto points from INY-134 (n = 16). The age of cat. no. 141 was excluded by Chauvenet's criterion.

Table 8. Measured metrics for INY-134 projectile points.

CODE	DEFINITION	UNITS
ML	Maximum length	mm
AL	Axial length	mm
SL	Stem length	mm
BI	Basal indentation	mm
MW	Maximum width	mm
BW	Basal width	mm
NW	Neck width	mm
MT	Maximum thickness	mm
LMW	Length at maximum width (measured from base)	mm
WT	Weight	g
DSA	Distal shoulder angle	degrees
PSA	Proximal shoulder angle	degrees
NOA	Notch opening angle	degrees

content varies between obsidian sources. However, it also varies within a source, sometimes significantly (Stevenson et al. 1993). This is understandable, since obsidian is a result of natural phenomena, not of a controlled industrial process, and different parts of a magma source may out-gas at differing rates. Thus, hydration rate variations are expected, and can account for outliers in the data. The implication for practical analysis is that one must be cautious about attributing significance to a single point. When drawing conclusions, the data must be considered in the aggregate, trends identified, and multiple sources of data integrated to reinforce the conclusions.

METRICS

The measurement methodology generally followed that of Thomas (1981), with some modifications as suggested by Basgall and Hall (2000). The measured metrics are defined in Table 8, and computed metrics are in Table 9. Codes used to describe damaged or incomplete points are in Table 10.

Table 9. Computed metrics for INY-134 projectile points.

CODE	DEFINITION	FORMULA
BIR	Basal indentation ratio	AL / ML
LWR	Length-to-width ratio	ML / MW
MWP	Maximum width percent	LMW / ML
BWMW	Basal width relative to maximum width	BW / MW

Table 10. Condition codes for projectile points.

CODE	DEFINITION	IMPLICATION	STATISTICAL USE
CMP	Complete	Dimensions reliable	All metrics included
DEB	Distal end broken	Length and weight unreliable	Not included in statistics
EAB	Ear broken	Basal width unreliable	Not included in statistics
SHB	Shoulder broken	Maximum width unreliable	Not included in statistics
TB	Tip broken	Very small loss	Use length dimensions with caution
BB	Base broken	Length, basal dimensions, weight unreliable	Not included in statistics
BF	Basal fragment	Length and weight unreliable	Not included in statistics
PLF	Potlidding on face	Thickness unreliable	Not included in statistics

Table 11. Reliability of projectile point metrics.

CATEGORY	METRICS	RANKING
I	NW, MT, BI, NOA, BW	Most reliable
II	SL, MW, PSA	Less reliable
III	AL, SL, WT, DSA	Least reliable

Dimensions of projectile points are subject to modification over time, as points were used, damaged, and resharpened (or reworked entirely). Length (maximum and axial) is most likely affected by such activities, as is distal shoulder angle; weight is also unreliable since major rework reduces weight. Somewhat less subject to alteration are stem length, maximum and basal width, and proximal shoulder angle. Since points were undoubtedly reworked while still hafted, the most stable metrics are neck width, notch opening angle, basal indentation, and thickness. Comparison analyses place greater weight on the more reliable metrics and de-emphasize the less reliable ones (Table 11).

The assemblage includes 31 Pinto points, all of which are obsidian. Metrics and statistics are in Table 12, and statistics are summarized in Table 13. There are no evident temporal trends in the metrics; of the 17 Pinto points which were dated by obsidian hydration, plotting the reliable metrics (NW, MT, BI, NOA) against age yielded values of $R^2 < 0.03$.

Basgall and Hall (2000) reported a study of bifurcate-stemmed points from 11 different sites in eastern California and central Nevada. Seven of them were from the western Great Basin (Alabama Gates [AG], Stahl site [SS], Pinto Basin [PB], Silent Snake [SS], Surprise Valley [SV], Monitor Valley [MV], and Hidden Cave [HC]. They also included four sites from Ft. Irwin (Goldstone [GS], Awl site [AW], Rogers Ridge [RR], and Floodpond [FP]). When the statistics of the Ayers Rock Pinto points are compared with these sites, using a t-test, the results are as shown in Table 14. The threshold for distinguishability at the 95 percent confidence level is 1.96; bold-faced type indicates the results are distinguishable.

SIMILARITY ANALYSIS

A score can be constructed to rank similarity among Pinto points from various sites, by counting the number of metrics which are indistinguishable in each category. An overall score is computed as a weighted sum of the category scores, using weights of w = 4 for Category I, w = 2 for Category II, and

Table 12. Pinto point metrics, INY-134.

Cat. No.	ML (mm)	AL (mm)	SL (mm)	BI (mm)	LMW (mm)	MW (mm)	BW (mm)	NW (mm)	MT (mm)	WT (g)	DSA (deg.)	PSA (deg.)	NOA (deg.)	BIR	LWR	MWP	WBWM	Cond. Code	Remarks
56	49.5*	45.2*	18.2	4.3	29.2	29.4	23.1	21.3	9.5	14.7	182	97	85	--	--	--	0.79	*DEB	
57	45.4	43.1	8.5	2.3	12.1	26.6	17.7	17.2	7.4	7.3	184	85	99	0.95	1.71	0.27	0.67	CMP	
60	40.8*	36.0*	11.9	4.8	17.0	30.2	15.5	14.5	8.2	10.1	200	98	102	--	--	--	0.51	*DEB	Unfinished?
61	45.0	40.5	10.5	4.5	13.2	27.2	21.0	18.2	7.5	7.0	215	109	106	0.90	1.65	0.29	0.77	CMP	Unfinished?
62	38.9	36.8	9.0	2.1	12.8	25.5	17.8*	15.3	9.7	7.9	206	112	94	0.95	1.53	0.33	--	EAB	
73	42.9	38.6	10.5	4.3	15.3	29.7	-	22.7	7.9	8.6	181	112	69	0.90	1.44	0.36	--	TB, EAB	
74	50.4	46.8	11.0	3.6	13.0	32.5	25.9	24.3	7.9	11.0	180	108	72	0.93	1.55	0.26	0.80	CMP	
116	34.6	32.9	9.3	1.7	16.2	23.4	13.9	12.9	7.5	5.4	215	106	109	0.95	1.48	0.47	0.59	TB	
137	34.7*	--	19.4	--	--	--	28.5	26.9	9.5	8.9	195	99	96	--	--	--	--	*DEB	
141	38.1	34.9	11.7	3.2	19.3	25.8	18.8	14.6	8.6	6.9	192	110	82	0.92	1.48	0.51	0.73	*DEB, SIB	
142	42.7	37.4	10.4	5.3	13.0	32.4	21.0	22.2	7.9	9.2	198	78	120	0.88	1.32	0.30	0.65	EAB	
143	53.0	50.1	13.6	2.9	19.5	31.6	22.7	21.2	9.5	13.7	215	106	109	0.95	1.68	0.37	0.72	CMP	
144	50.1	44.1	13.5	6.0	18.5	26.3	22.6	22.6	7.9	9.5	203	98	105	0.88	1.90	0.37	0.86	CMP	
147	55.1*	50*	14.5	5.1	18.9	26.8	22.1	17.8	10.4	13.1	180	117	63	--	--	--	0.82	*DEB	
153	46.6	42.7	9.2	3.9	25.1	27.8	19.7	18.4	6.7	8.2	185	100	85	0.92	1.68	0.54	0.71	TB	Unfinished?
157	49.2	43.7	11.7	5.5	18.7	34.2	21.3	18.9	7.6	10.4	194	105	89	0.89	1.44	0.38	0.62	CMP	
163	46.1	41.3	11.0	4.8	13.3	29.8*	23.1	24.6	12.6	13.9	202	88	114	0.90	--	0.29	--	*SHB	Unfinished?
168	48.6	45.0	9.6	3.6	16.7	28.9	23.7	20.9	8.8	10.2	202	108	94	0.93	1.68	0.34	0.82	CMP	
171	46.8	40.0	11.2	6.8	15.1	28.0	22.9	21.8	9.7	10.9	205	97	108	0.85	1.67	0.32	0.82	TB, *EAB	
172	62.2	58.7	11.0	3.5	19.7	28.1	21.1	18.8	6.7	9.8	208	102	106	0.94	2.21	0.32	0.75	TB	
173	43.9	41.5	10.0	2.4	18.5	23.5	18.2	17.8	8.8	8.3	219	95	124	0.95	1.87	0.42	0.77	TB	Unfinished?
174	55.6	50.5	13.1	5.1	15.0	36.4	25.7	24.2	9.3	14.2	168	102	66	0.91	1.53	0.27	0.71	CMP	
175	51.6	46.0	13.2	5.6	13.0	31.6*	24.3	24.3	13.6	16.9	180	90	90	0.89	--	0.25	--	TB, *SHB	Unfinished?
176	50.0	45.7	9.5	4.3	16.9	28.4	22.6	21.6	8.5	10.7	212	93	119	0.91	1.76	0.34	0.80	CMP	
177	52.1	47.6	16.5	4.5	20.1	34.6	23.8	22.6	8.7	13.9	197	105	92	0.91	1.51	0.39	0.69	TB, EAB	
178	45.9*	41.9*	10.2	4.0	19.7	34.5	21.3	19.0	6.2	8.6	177	108	69	--	--	--	0.62	*DEB	
179	27.2	25.6	9.9	1.6	11.6	23.5*	18.8	15.8	7.8	3.8	196	112	84	0.94	--	0.43	--	TB, *SHB	
180	61.8	56.2	13.0	5.6	27.5	29.3	19.3	19.9	15.7	17.7	223	83	140	0.91	2.11	0.44	0.66	TB	
181	46.2*	43.1*	12.3	3.1	20.5	28.0	19.6	15.7	9.8	10.7	208	114	94	--	--	--	0.70	*DEB	Unfinished?
210	29.8	27.7	7.5	2.1	14.1	18.7*	14.1	12.6	5.4	2.6	202	105	97	0.93	--	0.47	--	*SHB	Unfinished?

Table 13. Pinto point metrics summary, INY-134.

	ML (MM)	AL (MM)	SL (MM)	BI (MM)	LMW (MM)	MW (MM)	BW (MM)	NW (MM)	MT (MM)	WT (G)	DSA (DEG.)	PSA (DEG.)	NOA (DEG.)	BIR	LWR	MWP	WBWM
n	24	24	30	29	29	25	28	30	30	30	30	30	30	24	20	24	23
Mean	46.36	42.39	11.47	4.01	16.94	29.15	21.08	19.56	8.82	9.98	198.00	101.55	96.45	0.92	1.66	0.36	0.72
SD	19.43	17.75	2.49	1.56	4.92	11.65	6.37	3.79	2.16	3.47	14.08	9.84	18.47	0.35	0.80	0.16	0.32
Max	62.20	58.70	19.40	6.80	27.50	36.40	28.50	26.90	15.70	17.70	223.00	117.00	140.00	0.95	2.21	0.54	0.86
Min	27.20	25.60	7.50	1.60	11.60	23.40	13.90	12.60	5.40	2.60	168.00	78.00	63.00	0.85	1.32	0.25	0.51

Table 14. Results of t-test comparing Pinto points from INY-134 with other sites.

	Category I – Most Reliable				Category II – Less Reliable				Category III – Least Reliable			
Site	**BI**	**NW**	**MT**	**NOA**	**SL**	**PSA**	**MW**	**BW**	**ML**	**AL**	**WT**	**DSA**
Stahl	**3.53**	0.48	**2.58**	1.08	**2.56**	**2.89**	1.34	0.78	1.66	1.44	**3.97**	**3.25**
Alabama Gates	**4.81**	**5.16**	**4.29**	**3.63**	**2.90**	**3.33**	**3.89**	**2.71**	**4.30**	**4.15**	**7.79**	**6.49**
Pinto Basin	**7.78**	**5.08**	**2.91**	**5.02**	**2.55**	0.60	**3.53**	**3.36**	**3.46**	**3.11**	**6.72**	**6.65**
Silent Spring	1.01	**7.29**	**8.00**	**5.32**	**5.73**	**3.49**	1.45	**5.49**	0.72	0.98	**5.38**	**9.04**
Surprise Valley	**2.31**	**5.75**	**7.39**	ND	**4.29**	**3.32**	**3.18**	**6.56**	1.24	1.67	**10.53**	**2.87**
Monitor Valley	**3.21**	**9.37**	**9.26**	1.67	**6.14**	**4.38**	**2.76**	**6.88**	**1.96**	1.81	**10.09**	**4.62**
Hidden Cave	**3.89**	**10.17**	**7.11**	**3.12**	**7.06**	**6.16**	**3.31**	**8.25**	0.42	0.08	**7.65**	**7.49**
Awl	1.76	**2.11**	**2.34**	**2.42**	1.20	**1.96**	1.86	1.10	0.54	0.61	1.37	**4.70**
Goldstone	**2.14**	1.95	**2.11**	**3.36**	**2.25**	0.53	**2.07**	0.73	0.12	0.00	1.60	**3.57**
Rogers Ridge	**2.72**	**3.98**	**3.56**	**4.82**	0.99	0.20	**2.88**	**2.39**	**2.23**	**2.31**	**5.42**	**6.04**
Flood Pond	**3.11**	**2.94**	**3.78**	**3.31**	0.34	**2.36**	**2.84**	1.49	**2.82**	**2.82**	**4.94**	**5.20**

Table 15. Similarity scores, INY-134 Pinto points vs. other sites.

Site	Category I	Category II	Category III	Total
Stahl	15	2	2	19
Awl	10	6	3	19
Goldstone	10	2	3	15
Silent Snake Spring	5	2	2	9
Flood Pond	5	2	--	7
Monitor Valley	5	--	1	6
Rogers Ridge	--	4	--	4
Pinto Basin	--	2	--	2
Surprise Valley	--	0	2	2
Hidden Cave	--	0	2	2
Alabama Gates	--	--	--	--

w = 1 for Category III. Table 15 shows the scores, ranked in order of decreasing overall similarity; scores are plotted in Figure 7, showing both the overall score and a score based only on the most reliable (Category I) metrics. (Changing the choice of weighting factors changes the scores but not the ranking.) Examination of Figure 7 shows a considerable break in score between the top three sites and the rest. The score based on Category I metrics shows a significant drop between the top scoring site (Stahl) and the next two (Awl and Goldstone), with an equally large drop between the latter two and the rest. In either case, there is a fairly strong similarity between INY-134 on one hand and the Stahl site (INY-382), the Awl site (SBR-4562), and the Goldstone site (SBR-2348) on the other.

Two parameters which might be expected to impact the similarity are proximity between sites and the materials used in projectile point manufacture. Proximity would suggest possible cultural contact, including possible co-use of the sites, while materials constraints can obviously affect point morphology. Table 16 lists the sites with distance from INY-134 (Ayers Rock), and the percentage of points which were obsidian. Distance is not a minimum-cost computation, but is a simple geometric estimate from Figure 1 of Basgall and Hall (2000:239). Percent obsidian was computed from Basgall and Hall (2000:258, Table 6) as well.

Figure 8 shows the variation of similarity score with distance from INY-134. Clearly there is no consistent pattern; the highest score was obtained for the nearby Stahl site and the distant Awl and Goldstone sites. The nearby Alabama Gates site shows the least similarity.

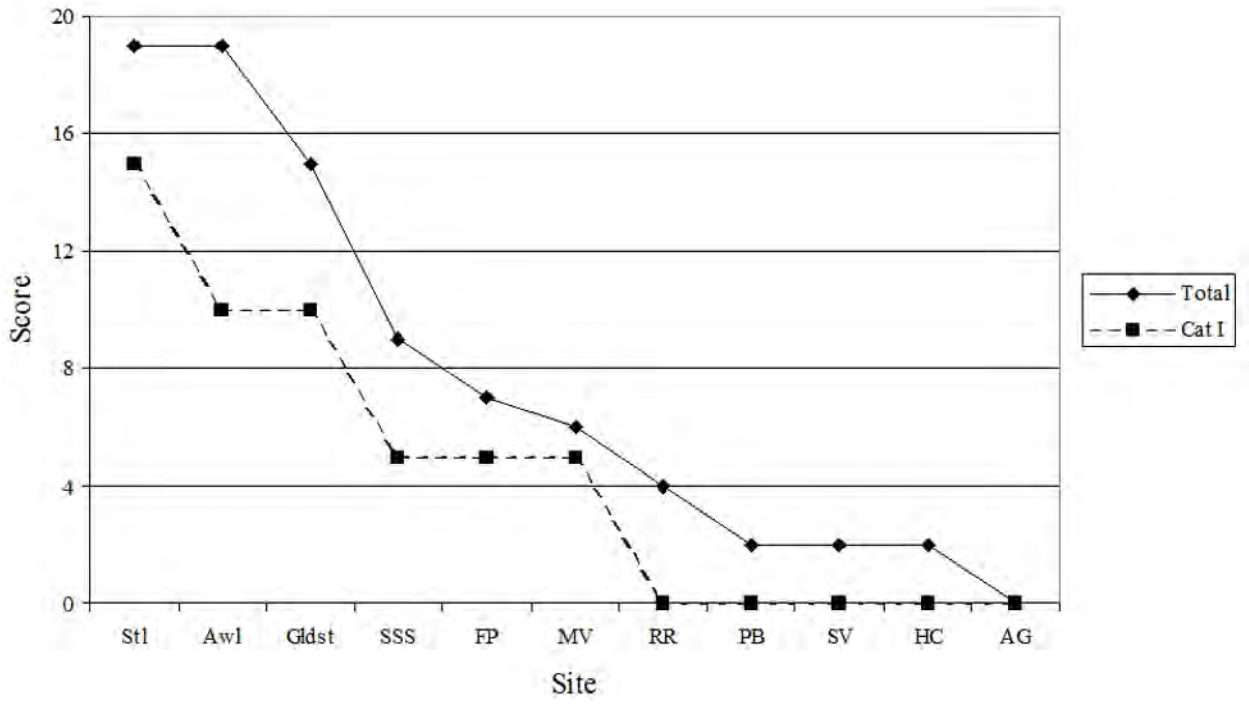

Figure 7. Similarity scores between INY-134 Pinto points and Pinto points at other sites.

Table 16. Pinto point similarity, distance, and percent obsidian.

SITE	SIMILARITY SCORE	DISTANCE (KM)	% OBSIDIAN
Ayer's Rock			100
Stahl	19	15	90
Awl	19	150	42
Goldstone	15	150	15
Silent Snake Spring	9	620	14
Flood Pond	7	150	23
Monitor Valley	6	350	6
Rogers Ridge	4	150	16
Pinto Basin	2	300	6
Surprise Valley	2	610	99
Hidden Cave	2	380	70
Alabama Gates	0	40	94

Distance estimated from Basgall and Hall (2000: 239, Fig. 1).
Percent obsidian computed from Basgall and Hall (2000:258, Table 6).

A similar conclusion applies to the effects of manufacturing materials on similarity score. Figure 9 shows the similarity score as a function of percent obsidian in the Pinto assemblage. Again, there is no consistent trend.

DISCUSSION

Several interesting questions arise from a consideration of the projectile point assemblage from Ayers Rock. What are the implications of the Pinto point metrics? Was there a Pinto-age occupation at all, or were the points curated?

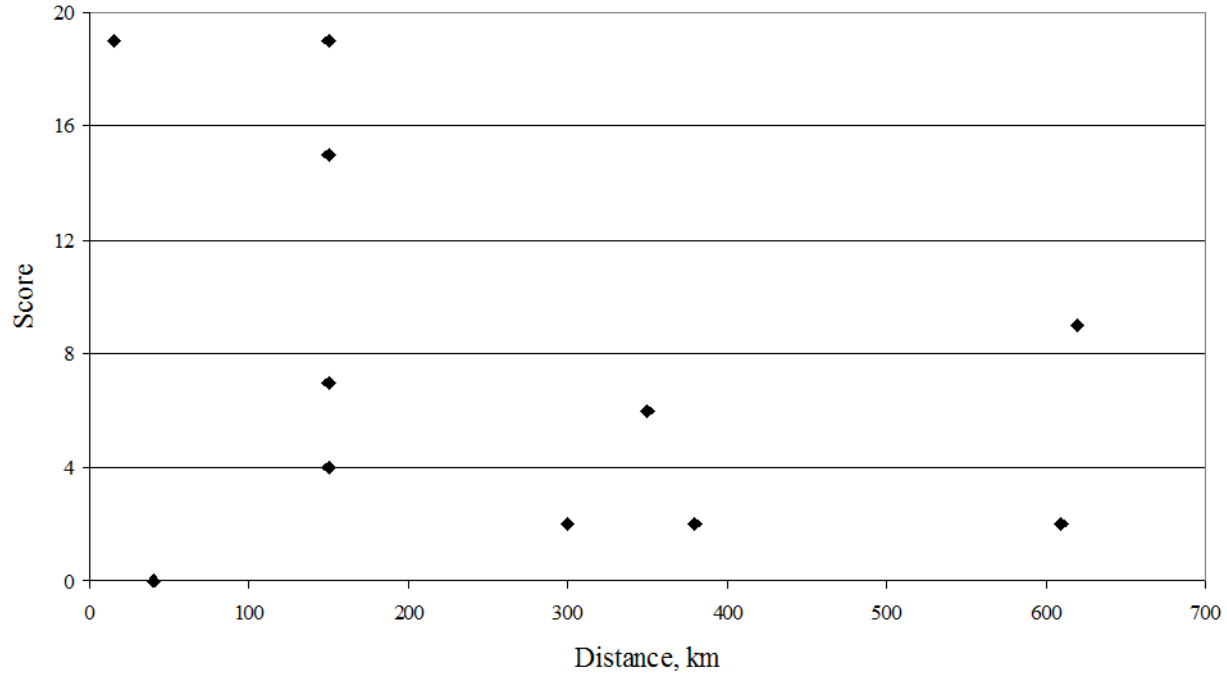

Figure 8. Variation of similarity score with distance from site to INY-134.

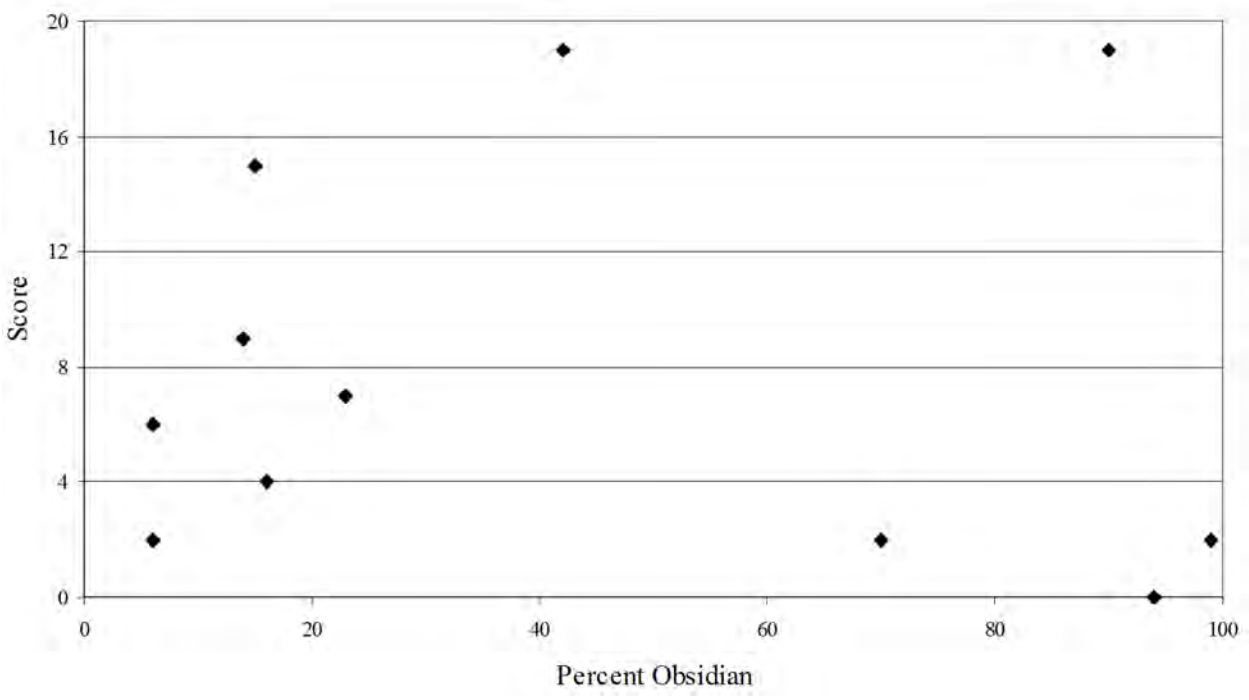

Figure 9. Dependence of similarity score on percent obsidian in Pinto point assemblages.

The customary assessment of the Pinto period is that it was warm and xeric (Warren and Crabtree 1986), and the inhabitants of the desert regions were widely dispersed near water sources (Sutton et al. 2007). A collector subsistence strategy is likely, with base camps tethered to water sources and logistic journeys to gather resources (Gardner 2006; Sutton et al. 2007).

Basgall and Hall (2000) compared Pinto point metrics from 11 sites in the southwestern Great Basin and Mojave Desert; however, their data set did not include Ayers Rock. The Pinto point metrics for Ayers Rock show that they are most similar to those of Stahl site (INY-182) Pinto points; however, the site with least similarity is the Alabama Gates site, which is nearby. Thus, there is no consistent variation of similarity with distance.

Obsidian is the material of choice for nearby sites (100 percent at Ayers Rock; 90 percent at Stahl), perhaps because of proximity to the Coso Volcanic Field. However, material choice does not fully explain the similarity, because the sites next most similar to Ayers Rock are the Awl site (SBR-4562) and Goldstone (SBR-2348), where the predominant material is basalt or cryptocrystalline silica. There is no consistent variation of similarity with distance.

Perhaps a better explanation than material technology is cultural affinity or cultural contact, a point which has not been explored heretofore. Ayers Rock and the Stahl site are nearby, so cultural contact was feasible. Further, Little Lake, which adjoins the Stahl site, has been a lake or wetland since the early Newberry period, and very likely before that (Mehringer and Sheppard 1978). Since there is no source of perennial water at Ayers Rock, the water at the Stahl site would have been an obvious incentive for contact.

The distance between Ayers Rock on the one hand and the Awl and Goldstone sites on the other hand is about 150 km. This is a significant distance, but probably within the logistic range of hunter-gatherer obsidian procurement (Beck and Jones 2011; Hildebrandt and Rosenthal 2014; Jones et al. 2012) or trade/exchange (Kelly 2011; King et al. 2011). Further, the Pinto period was one of significant drought in the Mojave Desert (Sutton et al. 2007). At such a time, the relatively abundant water in the canyons of the eastern Sierra Nevada, and probably at Little Lake, would have been attractive. This possibility has not been explored.

Was there a Pinto-age occupation at Ayers Rock? The site yielded a significant number of Pinto points, which led Whitley et al. (2005) to postulate such an occupation. However, the stratigraphic data raise questions. Examination of the stratigraphic distribution of projectile points shown in Figure 5 suggests that there is no evident stratigraphic separation between Pinto points and other point types. This impression is confirmed by the Kolmogorov-Smirnov analysis, which shows that the Pinto and Rose Spring distributions are not distinguishable.

If it could be shown that the distribution of the “arrow point” types (Desert series, Rose Spring, and Eastgate) was statistically distinguishable from Elko points, but not from Pinto, then one could conclude that the Pinto points were the result of curation during the Haiwee/Marana periods and there was no Pinto occupation. Unfortunately, 29 out of 31 Pinto points came from Shelter 1, and the sample size for the Elko points from Shelter 1 is too small to permit a valid statistical conclusion. On the other hand, the obsidian hydration dates on a large sample of Pinto points from the site yielded a mean age of 5684 ±1445 cal B.P., which is a valid Pinto period age (Haynes 2004).

Bacon et al. (2006) have reconstructed lake levels in Owens Lake, immediately north of Ayers Rock, and found that the lake was completely desiccated between approximately 6600 and 4400 cal B.P. This corresponds to the Pinto period, and suggests dry conditions throughout the southern region of the eastern Sierra Nevada and southwestern Great Basin. It is unlikely that Ayers Rock was an attractive place to live during such a period, especially since there is no evident source of perennial water near the site. On the other hand, the presence of high-quality obsidian for tool stone could have been a powerful draw for prehistoric populations, and water was available at Little Lake and the Sierra Nevada canyons. Given the proximity to the known Pinto-age occupation at Little Lake (Stahl site, INY-182), a Pinto-age occupation at Ayers Rock as suggested by Whitley et al. (2005) is not unlikely.

REFERENCES CITED

Ambrose, W. R., and C. M Stevenson

2004 Obsidian Density, Connate Water, and Hydration Dating. *Mediterranean Archaeology and Archaeometry* 4(2):5-16.

Anovitz, Lawrence M., David R. Cole, and Mostafa Fayek

2008 Mechanisms of Rhyolitic Glass Hydration below the Glass Transition. *American Mineralogist* 93:1166-1178.

Anovitz, Lawrence M., J. Michael Elam, Lee R. Riciputi, and David R. Cole

1999 The Failure of Obsidian Hydration Dating: Sources, Implications, and New Directions. *Journal of Archaeological Science* 26:735-752.

2004 Isothermal Time-Series Determination of the Rate of Diffusion of Water in Pachuca Obsidian. *Archaeometry* 42(2):301-326.

Bacon, Steven N., Raymond M. Burke, Silvio K. Pezzopane, and Angela S. Jayko

2006 Last Glacial Maximum and Holocene Lake Levels of Owens Lake, Eastern California, USA. *Quaternary Science Reviews* 25:1264-1282.

Basgall, Mark E., and M. C. Hall

2000 Morphological and Temporal Variation in Bifurcate-Stemmed Dart Points of the Western Great Basin. *Journal of California and Great Basin Anthropology* 22:237-276.

Beck, Charlotte, and George T. Jones

2011 The Role of Mobility and Exchange in the Conveyance of Toolstone during the Great Basin Paleoarchaic, pp. 55-82. In *Perspectives on Prehistoric Trade and Exchange in California and the Great Basin,* edited by Richard E. Hughes, pp. 55-82. University of Utah Press, Salt Lake City.

Carslaw, H. S., and J. C. Jaeger

1959 *Conduction of Heat in Solids,* 2nd ed. Clarendon Press, Oxford.

Cole, Franklyn W.

1970 *Introduction to Meteorology*. Wiley, New York.

Crank, John

1975 *The Mathematics of Diffusion*. Oxford University Press, Oxford.

Delaney, J. R., and J. L Karsten.

1981 Ion Microprobe Studies of Water in Silicate Melts: Concentration-dependent Water Diffusion in Obsidian. *Earth and Planetary Science Letters* 52: 191-202.

Doremus, Robert H.

2002 *Diffusion of Reactive Molecules in Solids and Melts*. Wiley Interscience, New York.

Ebert, W. L., R. F. Hoburg, and J. K. Bates

1991 The Sorption of Water on Obsidian and a Nuclear Waste Glass. *Physics and Chemistry of Glasses* 34(4):133-137.

Friedman, Irving, and Clifford Evans

1968 Obsidian Dating Revisited. *Science* 162:813-814.

Friedman, Irving, and W. D. Long

1976 Hydration Rate of Obsidian. *Science* 191:347-352.

Friedman, Irving, and R. Smith

1960 A New Method of Dating Using Obsidian: Part 1, the Development of the Method. *American Antiquity* 25:476-522.

Friedman, Irving, Robert I. Smith, and William D. Long

1966 Hydration of Natural Glass and Formation of Perlite. *Geological Society of America Bulletin* 77:323-328.

Friedman, Irving, F. W. Trembour, F. L. Smith, and G. I. Smith
1994 In Obsidian Hydration Affected by Relative Humidity? *Quaternary Research* 41(2):185-190.

Gardner, Jill K.
2006 The Potential Impact of the Medieval Climatic Anomaly on Human Populations in the Western Mojave Desert. Unpublished Ph.D. dissertation, Department of Anthropology, University of Nevada, Las Vegas.

Haynes, Gregory M.
2004 An Evaluation of the Chronological Relationships between Great Basin Stemmed and Pinto Series Projectile Points in the Mojave Desert. In *The Human Journey and Ancient Life in California's Deserts: Proceedings from the 2001 Millennium Conference*, edited by Mark. W. Allen and Judyth Reed, pp. 117-128. Maturango Museum Publication No. 15. Ridgecrest, California.

Hildebrandt, William R., and Jeffrey S. Rosenthal
2014 Reassessment of Early Holocene Mobility and Social Organization in the Great Basin. Paper presented at the 48th annual meeting of the Society for California Archaeology, Visalia.

Johnson, Michael J., Charles J. Mayers, and Brian J. Andraski
2002 *Selected Micrometeorological and Soil-Moisture Data at Amargosa Desert Research Site in Nye County near Beatty, Nevada, 1998 – 2000.* U.S. Geological Survey Open-File Report 02-348. USGS, Carson City, Nevada.

Jones, George T., Lisa M. Fontes, Rachel A. Horowitz, Charlotte Beck, and David G. Bailey
2012 Reconsidering Paleoarchaic Mobility in the Central Great Basin. *American Antiquity* 77:351-367.

Justice, Noel D.
2002 *Stone Age Spear and Arrow Points of California and the Great Basin*. Indiana University Press, Bloomington.

Karsten , J. L., J. R. Holloway, and J. L. Delaney
1982 Ion Microprobe Studies of Water in Silicate Melts: Temperature-dependent Water Diffusion in Obsidian. *Earth and Planetary Science Letters* 59:420-428.

Kelly, Robert L.
2011 Obsidian in the Carson Desert: Mobility or Trade? In *Perspectives on Prehistoric Trade and Exchange in California and the Great Basin*, edited by Richard E. Hughes, pp. 201-220. University of Utah Press, Salt Lake City.

King, Jerome, William R. Hildebrandt, and Jeffrey S. Rosenthal
2011 Evaluating Alternative Models for the Conveyance of Bodie Hills Obsidian into Central California. In *Perspectives on Prehistoric Trade and Exchange in California and the Great Basin*, edited by Richard E. Hughes, pp. 148-170. University of Utah Press, Salt Lake City.

Mazer, J. J., C. M. Stevenson, W. L. Ebert, and J. K. Bates
1991 The Experimental Hydration of Obsidian as a Function of Relative Humidity and Temperature. *American Antiquity* 56:504-513.

Mehringer, Peter J., and John C. Sheppard
1978 Holocene History of Little Lake, Mojave Desert, California. In *The Ancient Californians: Rancholabrean Hunters of the Mojave Lakes Country*, edited by Emma Lou Davis, pp. 153-166. Natural History Museum of Los Angeles County Science Series No. 29. Los Angeles.

Morgenstein, M. E, C. L. Wickett, and A. Barkett
1999 Considerations of Hydration-Rind Dating of Glass Artefacts: Alteration Morphologies and Experimental Evidence of Hydrogeochemical Soil-zone Pore Water Control. *Journal of Archaeological Science* 26:1193-1210.

Northwest Research Obsidian Studies Laboratory
2008 *Report NWROSL 2008-14*. Northwest Research Obsidian Studies Laboratory, Corvallis, Oregon.

Redfeldt, Gordon
1962 Painted Rock Site, Little Lake, California. *Newsletter of the Archaeological Survey Association of Southern California*. 9(2):4-5.

Riciputi, Lee R., J. M. Elam, L. M. Anovitz, and D. R. Cole
2002 Obsidian Diffusion Dating by Secondary Ion Mass Spectrometry: A Test Using Results from Mound 65, Chalco, Mexico. *Journal of Archaeological Scienc*e 29:1055-1075.

Rogers, Alexander K.
2007 Effective Hydration Temperature of Obsidian: A Diffusion-Theory Analysis of Time-Dependent Hydration Rates. *Journal of Archaeological Science* 34:656-665.
2008a Regional Scaling for Obsidian Hydration Temperature Correction. *Bulletin of the International Association for Obsidian Studies* 39:15-23.
2008b Field Data Validation of an Algorithm for Computing Effective Hydration Temperature of Obsidian. *Journal of Archaeological Science.* 35:441-447.
2008c An Evaluation of Obsidian Hydration Dating as a Chronometric Technique, Based on Data from Rose Spring (CA-INY-372), Eastern California. *Bulletin of the International Association for Obsidian Studies* 40:12-32.
2008d Obsidian Hydration Dating: Accuracy and Resolution Limitations Imposed by Intrinsic Water Variability. *Journal of Archaeological Science* 35:2009-2016.
2010a How Did Paleotemperature Change Affect Obsidian Hydration Rates? *Bulletin of the International Association for Obsidian Studies* 42:13-20.
2010b Accuracy of Obsidian Hydration Dating Based on Radiocarbon Association and Optical Microscopy. *Journal of Archaeological Science* 37:3239-3246.
2011 Do Flow-Specific Hydration Rates Improve Chronological Analyses? A Case Study for Coso Obsidian. *Bulletin of the International Association for Obsidian Studies* 45:14-25.
2012 Temperature Correction for Obsidian Hydration Dating. In *Obsidian and Ancient Manufactured Glasses*, edited by Ioannis Liritzis and Christopher Stevenson, pp. 46-56. University Of New Mexico Press, Albuquerque.

Rogers, Alexander K., and Daron Duke
2011 An Archaeologically Validated Protocol for Computing Obsidian Hydration Rates from Laboratory Data. *Journal of Archaeological Science* 38:1340-1345.

Schiffer, Michael B.
1987 *Site Formation Processes of the Archaeological Record*. University of Utah Press, Salt Lake City.

Stevenson, Christopher M., I. M. Abdelrehim, and S. W. Novak
2004 High Precision Measurement of Obsidian Hydration Layers on Artifacts from the Hopewell Site Using Secondary Ion Mass Spectrometry. *American Antiquity* 69:555-568.

Stevenson, Christopher M., J. Carpenter, and B. E. Scheetz
1998 Obsidian Dating: Recent Advances in the Experimental Determination and Application of Hydration Rates. *Archaeometry* 31:1193-1206.

Stevenson, Christopher M., Mike Gottesman, and Michael Macko
2000 Redefining the Working Assumptions for Obsidian Hydration Dating. *Journal of California and Great Basin Anthropology* 22:223-236.

Stevenson, Christopher M., Elizabeth Knauss, James J. Mazer, and John K. Bates
1993 The Homogeneity of Water Content in Obsidian from the Coso Volcanic Field: Implications for Obsidian Hydration Dating. *Geoarchaeology* 8(5):371-384.

Stevenson, Christopher M., James J. Mazer, and Barry E. Scheetz
1998 Laboratory Obsidian Hydration Rates: Theory, Method, and Application. In *Archaeological Obsidian Studies: Method and Theory. Advances in Archaeological and Museum Science*, Vol. 3, edited by M. S. Shackley, pp.181-204. Plenum Press, New York.

Stevenson, Christopher M., and Steven W. Novak
2011 Obsidian Hydration Dating by Infrared Spectroscopy: Method and Calibration. *Journal of Archaeological Science* 38:1716-1726.

Stevenson, Christopher M., and B. E. Scheetz
1989 Induced Hydration Rate Development of Obsidians from the Coso Volcanic Field: A Comparison of Experimental Procedures. In *Current Directions in California Obsidian Studies,* edited by Richard E. Hughes, pp. 23-30. Contributions of the University of California Archaeological Research Facility No. 48. Berkeley.

Sutton, Mark Q., Jill K. Gardner, and Mark W. Allen
2007 Advances in Understanding Mojave Desert Prehistory. In *California Prehistory: Colonization, Culture, and Complexity,* edited by Terry L. Jones and Kathryn A. Klar, pp. 229-246. Altamira Press, Lanham, Maryland.

Thomas, David Hurst
1981 How to Classify the Projectile Points from Monitor Valley, Nevada. *Journal of California and Great Basin Anthropology* 3:7-43.

Warren, Claude N., and Robert H. Crabtree
1986 Prehistory of the Southwest Area. In *Great Basin,* edited by Warren L. d'Azevedo, pp. 183-193. Handbook of North American Indians, Vol. 11, William C. Sturtevant, general editor. Smithsonian Institution, Washington, D.C.

West, G. James, Wallace Woolfenden, James A. Wanket, and R. Scott Anderson
2007 Late Pleistocene and Holocene Environments. In *California Prehistory: Colonization, Culture, and Complexity*, edited by Terry L. Jones and Kathryn A. Klar, pp. 11-34. Altamira Press, Lanham, Maryland.

Whitley, David S., Tamara K. Whitley, and Joseph M. Simon
2005 *The Archaeology of Ayers Rock (CA-INY-134), California*. Maturango Museum Publication No. 19. Ridgecrest, California.

Yohe, Robert M., II
1998 The Introduction of the Bow and Arrow and Lithic Resource Use at Rose Spring (CA-INY-372). *Journal of California and Great Basin Anthropology* 20:26-52.

Zhang, Youxue, and Harald Behrens
2000 H_2O Diffusion in Rhyolitic Melts and Glasses. *Chemical Geology* 169:243-262.

Zhang, Y., E. M. Stolper, and G. J. Wasserburg
1991 Diffusion of Water in Rhyolitic Glasses. *Geochimica et Cosmochimica Acta* 55:441-456.